Small cross section of the synthesis of darmstadtium in the ^{48}Ca + ^{232}Th reaction

A. K. Nasirov [1,2,*] A. R. Yusupov,[2,†] and B. M. Kayumov [2,3,‡]

[1]*Bogoliubov Laboratory of Theoretical Physics, Joint Institute for Nuclear Research, Dubna 141980, Russia*
[2]*Laboratory of Theoretical Nuclear Physics, Institute of Nuclear Physics, Tashkent 100214, Uzbekistan*
[3]*School of Humanities and Natural Sciences, New Uzbekistan University, Tashkent 100000, Uzbekistan*

(Received 22 May 2024; revised 12 June 2024; accepted 27 June 2024; published 22 July 2024)

The smallness of the cross section of evaporation residues formed in the hot fusion reaction ^{48}Ca + ^{232}Th is analyzed by the dinuclear system model (DNS). The capture probability has been calculated by solving the dynamical equations of motion for the relative distance between the centers of mass of the DNS nuclei. Fusion of nuclei is considered as evolution of the DNS to a stable compound nucleus. The fusion probability has a bell-like shape and quasifission is one of reasons causing smallness of the yield of the evaporation residues products. Another reason is the decrease of the fission barrier for the isotopes $^{275-285}$Dm related with the shell effects in the neutron structure. The agreement of the theoretical results obtained for the yield of the evaporation residues with the experimental data measured in the Factory of Superheavy Elements of Joint Institute for Nuclear Research is well.

DOI: 10.1103/PhysRevC.110.014618

I. INTRODUCTION

The synthesis of new superheavy elements as a result of collisions of heavy nuclei is one of the important topics for many people interested in modern nuclear physics [1]. In recent years, new superheavy elements have been synthesized using heavy elements and actinide nuclei from the periodic table [2–4].

Currently, there is no theoretical model that fully explains the process of complete fusion in heavy ion collisions. Existing nuclear models are able to explain some features of this process. Several mechanisms are analyzed to explain the joining processes. To date, many theoretical studies have been carried out to calculate the evaporation residue (ER) cross sections in the complete fusion reaction at heavy ion collisions [5–9]. The cross section of the evaporation residue depends on the collision energy and orbital angular momentum of the entrance channel and the physical properties of the projectile-target pair. A knowledge about the fusion mechanism is very useful at the exploration of the optimal conditions for the synthesis of new superheavy elements. It is well known that the ER cross section of the heaviest elements is very small and its excitation function range is very narrow [2,10]. Only a narrow range of 15–20 MeV of the collision energy values corresponds to the observable excitation functions of synthesis of the superheavy elements. To determine the best conditions for the input channel during the synthesis of superheavy elements, theoretical calculations usually study the dependence of the evaporation cross section σ_{ER} on the collision energy ($E_{\rm c.m.}$), orbital angular momentum ($L = \ell\hbar$), and structure of colliding nuclei [5,11]:

$$\sigma_{ER}(E_{\rm c.m.}) = \sum_{\ell=0}^{\ell_d} \sigma_{\rm cap}(E_{\rm c.m.}, \ell) \times P_{\rm CN}(E_{\rm c.m.}, \ell) W_{\rm sur}(E_{\rm c.m.}, \ell), \quad (1)$$

where $P_{\rm CN}(E_{\rm c.m.}, \ell)$ is a hindrance factor to complete fusion [5,11], $\sigma_{\rm cap}(E_{\rm c.m.}, \ell)$ is partial capture cross section, and $W_{\rm sur}(E_{\rm c.m.}, \ell)$ is survival probability of the rotating and heated compound nucleus against fission by neutron emission.

It is important to estimate accurately the cross section of complete fusion leading to form a compound nucleus,

$$\sigma_{\rm fus}(E_{\rm c.m.}) = \sum_{\ell=0}^{\ell_d} \sigma_{\rm cap}(E_{\rm c.m.}, \ell) P_{\rm CN}(E_{\rm c.m.}, \ell). \quad (2)$$

In heavy ion collisions with massive nuclei the ER cross section is a very small part of the fusion cross section. The experimental value of $\sigma_{\rm fus}(E_{\rm c.m.})$ is determined as a sum of the cross sections of the measured yield of the reaction products of the fusion-fission and evaporation residue channels:

$$\sigma_{\rm fus}^{(\rm exp)}(E_{\rm c.m.}) = \sigma_{\rm fus.fis}^{(\rm exp)}(E_{\rm c.m.}) + \sigma_{\rm ER}^{(\rm exp)}(E_{\rm c.m.}). \quad (3)$$

It is well known that in some reactions the mass distribution of the fusion-fission products may overlap with the one of the quasifission products. In this case, it is necessary to separate pure fusion-fission products from quasifission products. It is an ambiguous task at the analysis of the measured data [12]. As a result the values of the fusion probability $P_{\rm CN}$ extracted from the measured data may be incorrect [13]. This creates uncertainty at the estimation of $P_{\rm CN}$ basing in the yield of

*Contact author: nasirov@jinr.ru
†Contact author: yanuclear009@gmail.com
‡Contact author: b.kayumov@newuu.uz

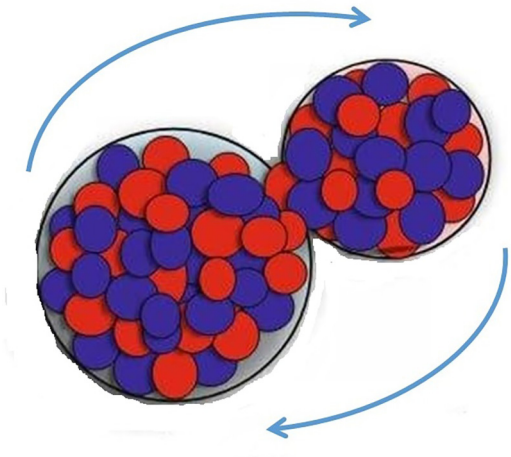

FIG. 1. The sketch of the nucleon transfer between fragments of the rotating DNS formed at capture of the projectile nucleus by the target nucleus.

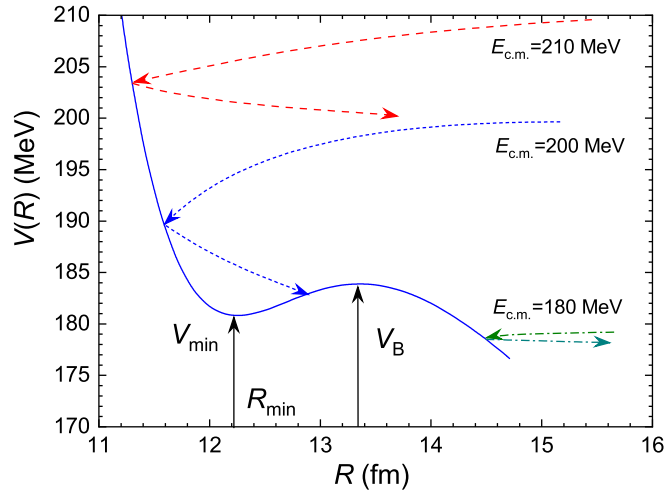

FIG. 2. The sketch of trajectories of the inelastic collisions (at $E_{\text{c.m.}} = 210$ and 180 MeV) and capture (at 200 MeV) is due to a decrease in the initial kinetic energy of collision under the influence of friction forces. The nuclear interaction potential $V(R)$ is shown by the solid curve.

the binary products. One of the reasons causing the smallness of the ER cross section is the dominance of the quasifission events in the reactions with the massive nuclei.

In this work, we used the DNS model for the description of the ER cross sections. According to the DNS model, a "neck" appears between the close surfaces of the projectile and the target nuclei and through this "neck" nucleons are transferred between nuclei (Fig. 1). During the process of the mutual transfer of nucleons, the nucleons occupy the empty quantum states of the acceptor nucleus [1].

The study of the fusion mechanism is also directly related with the potential energy surface (PES) of the system. It allows us to evaluate possible reaction channels and to estimate the excitation energy of the DNS. During the fusion process, nucleons move from the light nucleus to the heavy one. The motion of the nucleons takes place as a diffusion process, but the average flow goes in one or another direction as a function of the PES landscape which determines by the DNS angular momentum. Nucleon transfer changes the mass and charge distribution in the DNS fragments and there is a possibility of the DNS breakup which is considered as the quasifission process. Experimental and theoretical analysis of the yield of the products of the reactions with the massive nuclei shows that the process of quasifission is the dominant channel compared to complete fusion [12].

The main goal of this research work is to calculate the cross section of the capture, complete fusion and evaporation residue formation for the theoretical study of the synthesis of superheavy element $^{280-xn}$Ds in the $^{48}\text{Ca} + ^{232}\text{Th}$ reaction. In the recent experiments of the Flerov Laboratory of Nuclear Reaction of JINR (Dubna, Russia), the maximum values of the cross sections $0.7^{+1.1}_{-0.5}$ pb for the $4n$ channel [14] and $0.34^{+0.59}_{-0.16}$ for the $5n$ channel [15] of the evaporation residues at the synthesis of the element Ds have been measured. These cross sections are much smaller than the experimental data 15^{+9}_{-6} obtained in the cold fusion $^{64}\text{Ni} + ^{208}\text{Pb}$ reaction [16]. Note these cold and hot fusion reactions lead to the different isotopes of Ds. It is important for researchers to know the reasons unambiguously leading to this difference in the observed ER cross sections. Is it related with the formation of the compound nucleus and/or its survival probability against fission.

The process of synthesis of superheavy elements is considered as a final of the three stages. The first stage represents a competition between the deep-inelastic collision (this process occurs due to incomplete momentum transfer) and the capture process (this process occurs due to full momentum transfer). If the kinetic energy of the projectile is greater than the Coulomb barrier of the nucleus-nucleus interaction potential, deep inelastic collision or capture projectile by the target nucleus occurs after dissipation of the sufficient part of the relative kinetic energy. If the DNS is able to overcome the Coulomb barrier from the inside part the potential shell to outside then deep-inelastic collision takes place (Fig. 2). Otherwise, the DNS nuclei is captured by the potential interaction well. The last condition is called full momentum transfer. The competition between capture and deep-inelastic collisions depends on the charge and mass numbers of the colliding nuclei, relative energy, and orbital angular momentum of collision.

At the second stage of the evolution of the DNS there is a competition between formation of a compound nucleus (complete fusion of nuclei) or the DNS breakup into two parts without reaching the equilibrium state of the compound nucleus. At the last stage, the heated and rotating compound nucleus should survive against the fission process.

In this work involving the $^{48}\text{Ca} + ^{232}\text{Th}$ reaction, we calculated the cross sections for the capture of nuclei, fusion, and evaporation residue of the resulting compound nucleus depending on various energies and orbital angular momentum.

II. CAPTURE CROSS SECTION

Calculation of the capture probability of the projectile by target nucleus at energies near the Coulomb barrier is

performed by solution dynamical equations for the relative motion of the incoming trajectory of collision, as a result the capture cross section can be calculated by using the following equation:

$$\sigma_{\rm cap}(E_{\rm c.m.},\{\alpha_i\}) = \frac{\lambda^2}{4\pi}\sum_{\ell=0}^{\ell_d}(2\ell+1)P_{\rm cap}(E_{\rm c.m.},\ell,\{\alpha_i\}), \quad (4)$$

where λ is the de Broglie wavelength of the input channel and $P_{\rm cap}(E_{\rm c.m.},\ell;\ \{\alpha_i\})$ is the capture probability; ℓ_d is the dynamical maximum value of the orbital momentum leading to capture in collisions with the orientation angles α_i of the axial symmetry axis of colliding nuclei relative the beam direction. The capture probability $P_{\rm cap}$ can be equal to 1 or 0 for the given beam energy and orbital angular momentum. For the given energy the number of partial waves (ℓ_d) leading to capture is calculated by the solution of equations of the relative motion of nuclei [11,17]:

$$\frac{d\dot{R}}{dt} + \gamma_R(R,\alpha_1,\alpha_2)\dot{R}(t) = F(R), \quad (5)$$

$$F(R,\alpha_1,\alpha_2) = -\frac{\partial V(R,\alpha_1,\alpha_2)}{\partial R} - \dot{R}^2\frac{\partial\mu(R)}{\partial R}, \quad (6)$$

$$\frac{dL}{dt} = (\dot{\theta}R(t) - \dot{\theta}_1 R_{1\rm eff} - \dot{\theta}_2 R_{2\rm eff})\gamma_\theta(R,\alpha_1,\alpha_2)R(t), \quad (7)$$

$$L_0 = J_R(R,\alpha_1,\alpha_2)\dot{\theta} + J_1\dot{\theta}_1 + J_2\dot{\theta}_2, \quad (8)$$

$$E_{\rm rot} = \frac{J_R(R,\alpha_1,\alpha_2)\dot{\theta}^2}{2} + \frac{J_1\dot{\theta_1}^2}{2} + \frac{J_2\dot{\theta_2}^2}{2}, \quad (9)$$

where $R \equiv R(t)$ is the relative distance between centers of mass interacting nuclei; $\dot{R}(t)$ is the corresponding velocity; L_0 ($L_0 = \ell_0\hbar$) and $E_{\rm kin} = E_{\rm c.m.}$ at $R \to \infty$ are initial conditions; $\mu(R,\alpha_1,\alpha_2) = mA_PA_T/(A_P+A_T) + \delta\mu(R,\alpha_1,\alpha_2)$ [17], where $Z_P(A_P)$ and $Z_T(A_T)$ are charge (mass) numbers of the colliding nuclei, respectively, m is mass of nucleon; $J_R = \mu R^2$ and $J_i = A_i m(a_i^2 + b_i^2)/5$ are moments of inertia of the DNS and its fragments, respectively; $\dot{\theta}_i$ is the angular velocity of the fragment "i", $i = 1, 2$; $\dot{\theta}$ is the angular velocity of the whole DNS around its center of mass. γ_R and γ_θ are the friction coefficients for the relative motion along R and the tangential motion when two nuclei roll on each other's surfaces, respectively. Their values are determined from the estimation of the particle-hole excitation in nuclei and nucleon exchange between them [11,17,18]. $V(R,\alpha_1,\alpha_2) = V(Z_P,A_P,Z_T,A_T,R,\alpha_1,\alpha_2)$ is the nucleus-nucleus potential calculated by the double folding procedure [11,17] with the effective nucleon-nucleon forces suggested by Migdal [19].

Figure 2 shows the trajectories of deep-inelastic collisions at energies $E_{\rm c.m.} = 210$ and 180 MeV, according to the DNS model, when the full momentum transfer of the relative motion does not take place. In collisions with the energies around $E_{\rm c.m.} = 200$ MeV the full momentum transfer occurs, i.e., projectile nucleus is captured by the target nucleus. The kinetic energy is fully dissipated and the arrow of energy ends in the bottom of the well of the nucleus-nucleus interaction $V_{\rm min}(R_{\rm min},\ell,\{\alpha_i\})$ at the distance $R = R_{\rm min}$.

The depth of the interaction potential $B_{\rm qf} = V_B - V_{\rm min}$ is used in the DNS model as the quasifission potential. It determines the stability of the DNS against breakup into two parts (quasifission). Therefore, it is called a quasifission barrier (see Fig. 2). The size of the potential well depends on the mass and charge numbers of interacting nuclei, and on the orientation angles α_i of the symmetry axis of the deformed nucleus ($|\beta_i| > 0$) relative to the direction of the projectile velocity [$i = 1$ (projectile), 2 (target)] [17] and on the orbital angular momentum (ℓ).

For the given relative energy ($E_{\rm c.m.}$) and orbital angular momentum (ℓ), the capture cross section ($\sigma_{\rm cap}$) can be expressed as the sum of the competing channels cross sections:

$$\sigma_{\rm cap}(E_{\rm c.m.},\{\alpha_i\}) = \sigma_{\rm fus}(E_{\rm c.m.},\ell,\{\alpha_i\}) + \sigma_{\rm qfis}(E_{\rm c.m.},\ell,\{\alpha_i\}) + \sigma_{\rm ffis}(E_{\rm c.m.},\ell,\{\alpha_i\}), \quad (10)$$

where $\sigma_{\rm fus}$ is the cross section for complete fusion of nuclei; $\sigma_{\rm qfis}$ is the cross section for DNS quasifission, σ_{ffis} is the cross section for fast fission of the rotating mononuclear.

The potential well gives the possibility of capture. If the value of the orbital momentum and energy satisfy the following conditions: $\ell < \ell_d$ and $E_{\rm c.m.} > V_B$, then the capture probability $P_{\rm cap}$ is equal to unity. Conversely, if $\ell > \ell_d$ and $E_{\rm c.m.} > V_B$, then $P_{\rm cap}$ is equal to zero.

However, in the case $E_{\rm c.m.} < V_B(\ell)$ the capture process can occur due to the tunneling effect where the value of $E_{\rm c.m.}$ satisfies the condition $V_{\rm min}(\ell) < E_{\rm c.m.} < V_B(\ell)$ for any value of the ℓ-orbital angular momentum. Then the probability of the barrier penetrability $\mathcal{P}_{\rm tun}^{(\ell)}$ is calculated by the WKB formula obtained in Ref. [20]:

$$\mathcal{P}_{\rm tun}^{(\ell)}(E_{\rm c.m.},\{\alpha_i\}) = \frac{1}{1+\exp\left[2K(E_{\rm c.m.},\ell,\{\alpha_i\})\right]}, \quad (11)$$

where

$$K(E_{\rm c.m.},\ell,\{\alpha_i\}) = \int_{R_{\rm in}}^{R_{\rm out}} dR\sqrt{\frac{2\mu}{\hbar^2}(V(R,\ell,\{\alpha_i\}) - E_{\rm c.m.})}, \quad (12)$$

$R_{\rm in}$ and $R_{\rm out}$ are inner and outer turning points which were estimated by $V(R) = E_{\rm c.m.}$.

III. POTENTIAL ENERGY SURFACE AND DRIVING POTENTIAL

The main role in the formation and evolution of the DNS is played by the PES and dynamic coefficients (friction force and moment of inertia) [18]. PES is a function of the mass (A_i) and charge (Z_i) numbers of the colliding nuclei, the orbital angular momentum (ℓ) and the relative distance between their centers of mass, and can be calculated as a function of R (see Fig. 3):

$$U(Z,A,\ell,R,\{\alpha_i\}) = V(Z,A,\ell,R,\{\alpha_i\}) + Q_{gg} - V_{\rm rot}^{CN}, \quad (13)$$

where $Q_{gg}(Z,A) = B_1(Z,A) + B_2(Z_c,A_c) - B_{\rm CN}$ is the reaction balance energy; B_1, B_2, and $B_{\rm CN}$ are binding energies of the interacting nuclei $(Z,A;Z_c,A_c)$ of DNS and the compound nucleus with the charge $Z_{\rm CN}$ and mass $A_{\rm CN}$ numbers which

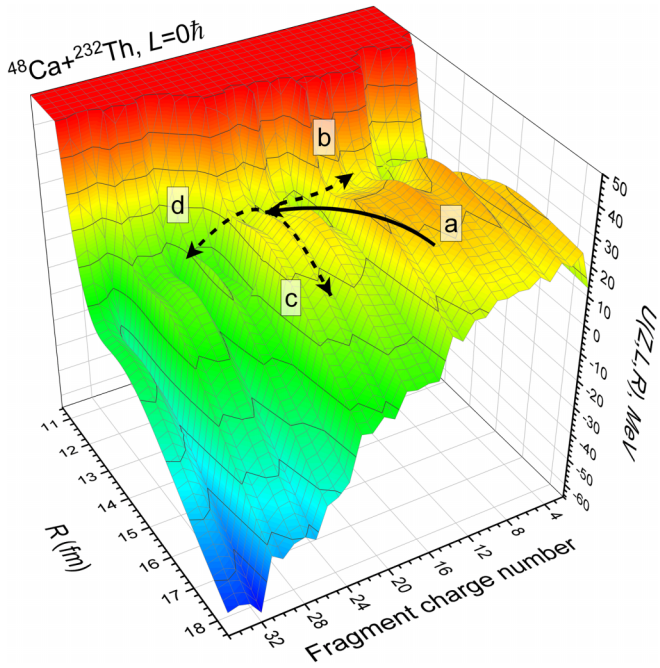

FIG. 3. The potential energy surface of the DNS formed in the reaction $^{48}\mathrm{Ca}+^{232}\mathrm{Th}$ calculated for collisions with the value of the orbital angular momentum $\ell = 0$ and the orientation angles $\alpha_1 = 30^\circ$ and $\alpha_2 = 135^\circ$. The arrow (a) shows the input capture channel; the arrow (b) shows the directions of the complete fusion by the nucleon transfer from a light nucleus to a heavy one; arrows (c) and (d) show the directions of the DNS decay into mass-asymmetric and symmetric quasifission channels, respectively.

is formed at complete fusion; their values are taken from the table in Refs. [21,22]; $Z_{\mathrm{CN}} = Z_P + Z_T$, $A_{\mathrm{CN}} = A_P + A_T$, $Z = Z_{\mathrm{CN}} - Z_c$, and $A = A_{\mathrm{CN}} - A_c$, where Z and A are charge and mass numbers of the light fragment of DNS and Z_c and A_c are the ones of the conjugate heavy fragment. The nucleus-nucleus interaction $[V(R)]$ between the projectile and the target nuclei consists of three parts:

$$V(Z,A;\ell,R,\{\alpha_i\}) = V_N(Z,A;R,\{\alpha_i\}) + V_C(Z,A;R,\{\alpha_i\}) + V_{\mathrm{rot}}(Z,A;\ell,R,\{\alpha_i\}), \quad (14)$$

where V_N, V_C, and V_{rot} are the nucleus-nucleus, Coulomb, and rotational potentials, respectively. Methods of calculation of the potentials V_N and V_C have been presented in Appendix A of Ref. [17], and the rotational part the nucleus-nucleus interaction V_{rot} is given by

$$V_{\mathrm{rot}}(Z,A;\ell,R,\{\alpha_i\}) = \frac{\ell(\ell+1)\hbar^2}{2\mu R^2 + J_1 + J_2}. \quad (15)$$

The potential energy surface $V(Z,A;R,\{\alpha_i\})$ with the showed directions of the possible evolution of the DNS formed in the reaction $^{48}\mathrm{Ca}+^{232}\mathrm{Th}$ is presented in Fig. 3 for the collision with $L = 0$, orientation angles $\alpha_1 = 30^\circ$ and $\alpha_2 = 135^\circ$. The arrow (a) shows the input capture channel; the arrow (b) shows the directions of the complete fusion by the nucleon transfer from a light nucleus to a heavy one; arrows (c) and (d) show the directions of the DNS decay into mass-asymmetric and

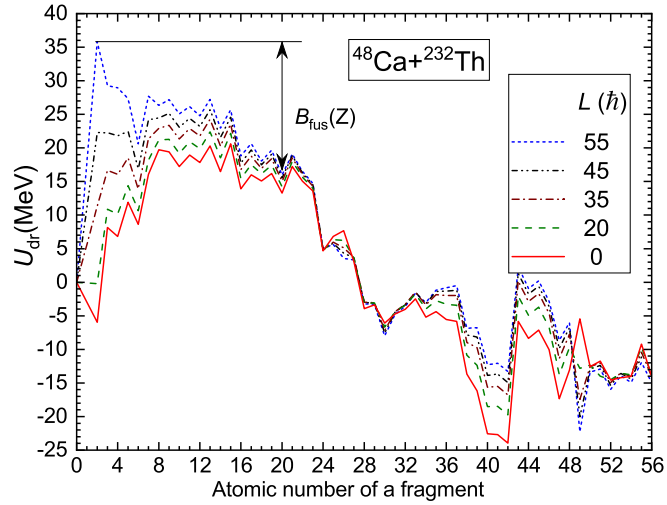

FIG. 4. The driving potential calculated for the $^{48}\mathrm{Ca}+^{232}\mathrm{Th}$ reaction for the orientation angles $\alpha_P = 30^\circ$ and $\alpha_T = 45^\circ$ of the axial symmetry of the nuclei of DNS formed with the angular momentum $L = 0, 20, 35, 45, 55\ \hbar$. $B^*_{\mathrm{fus}}(Z)$ is an internal nuclear barrier that causes hindrance to complete fusion for the charge asymmetry state $Z = 20$ of the DNS.

symmetric quasifission channels, respectively. When DNS break up into two fragments before (without) reaching an equilibrium state of compound nucleus after capture it is called quasifission.

The curve connecting of the minima of the PES valley is used as driving potential U_{dr} for the DNS formed in the given reaction

$$U_{dr}(Z,A,\ell,\{\alpha_i\}) = V(Z,A,\ell,R_{\mathrm{min}},\{\alpha_i\}) + Q_{gg} - V^{CN}_{\mathrm{rot}}. \quad (16)$$

In DNS model, the intrinsic fusion barrier B^*_{fus} for the fusion from the charge asymmetry Z of the DNS can be found from the peculiarities of U_{dr} as it is showed in Fig. 4 for the DNS with the angular momentum $L = 55\hbar$. Its values may vary depending on the deformation parameters $\{\beta_i\}$ of interacting nuclei and orientation angles $\{\alpha_i\}$.

IV. FUSION CROSS SECTIONS

The extraction of the fusion probability P_{CN} from the experimental data is an ambiguous procedure since there is a freedom in definition of the capture σ_{cap} and fusion σ_{fus} cross sections [12,13]:

$$P_{\mathrm{CN}}(E_{\mathrm{c.m.}}) = \sigma_{\mathrm{fus}}/(\sigma_{\mathrm{cap}} + \sigma_{\mathrm{fus}}). \quad (17)$$

This fact is related with the borders of the mass-energetic distributions of the capture events considered by the authors and possibility of the overlap of the mass distributions of the fusion-fission and quasifission products.

The theoretical fusion probability P_{CN} is calculated by the use of the intrinsic fusion barrier B^*_{fus}, which hinders complete fusion and quasifission barrier B_{qf}, which prevents the decay of DNS into two fragments. These barriers are determined

from the landscape of the potential energy surface and the estimation ways of them are shown in Figs. 3(b) and 3(c).

The fusion probability $P_{\rm CN}(E_{\rm c.m.}, \ell, \{\alpha_i\})$ depends on the change in mass and charge distributions of D_Z in DNS fragments after capture [23]. In general, it is calculated as the sum of the competing channel of quasifission and complete fusion at different charge asymmetries from the symmetric configuration $Z_{\rm sym}$ direction (d) in Fig. 3 of the DNS to the configuration corresponding to the maximum value of the driving potential $Z_{\rm max}$ and can be represented in this form

$$P_{\rm CN}(E_{\rm c.m.}, \ell, \{\alpha_i\}) = \sum_{Z_{\rm sym}}^{Z_{\rm max}} D_Z(E_Z^*, \ell, \{\alpha_i\}) P_{\rm CN}^{(Z)}(E_Z^*, \ell, \{\alpha_i\}). \tag{18}$$

The values of the $D_Z(E_Z^*, \ell, \{\alpha_i\})$ are calculated by the solution of the transport master equation with the nucleon transition coefficients depending on the occupation numbers and energies of the single-particle states of nucleons of the DNS nuclei [23]. The fusion probability $P_{CN}^{(Z)}(E_Z^*, \ell, \{\alpha_i\})$ for the DNS fragments with the charge configuration Z rotating with the orbital angular momentum ℓ is calculated as the branching ratio of the level densities of the quasifission barrier $B_{qf}^{(Z)}(\ell, \{\alpha_i\})$ at a given mass asymmetry, over the intrinsic barrier $B_{fus}^{*(Z)}(\ell, \{\alpha_i\})$ and symmetry barrier $B_{\rm sym}^{(Z)}(\ell, \{\alpha_i\})$ on mass asymmetry axis [24]:

$$P_{CN}^{(Z)}(\xi) = \frac{\rho_{\rm fus}(\xi)}{\rho_{\rm fus}(\xi) + \rho_{\rm qfiss}(\xi) + \rho_{\rm sym}(\xi)}, \tag{19}$$

where $\xi \equiv (E_Z^*, \ell, \{\alpha_i\})$ has been used for simplicity. The use of the level density function of the Fermi system leads to the formula for the fusion probability at the DNS excitation energy E_Z^* and angular momentum L from its charge asymmetry Z:

$$P_{CN}^{(Z)}(\xi) = \frac{e^{-B_{\rm fus}^{*(Z)}/T_Z}}{e^{-B_{\rm fus}^{*(Z)}/T_Z} + e^{-B_{\rm qf}^{(Z)}/T_Z} + e^{-B_{\rm sym}^{*(Z)}/T_Z}}. \tag{20}$$

Here, the values of the level density on the barriers $B_{\rm fus}^{(Z)*}(\alpha_i)$, $B_{\rm sym}^{*(Z)}(\alpha_i)$, and $B_{qf}^{(Z)}(\alpha_i)$ have been used. To simplify the presentation of Eqs. (19) and (20) the arguments (α_i) of the functions $E_Z^*(\alpha_i)$, $T_Z(\alpha_i)$, $B_{\rm fus}^{*(Z)}(\alpha_i)$, $B_{\rm sym}^{*(Z)}(\alpha_i)$, and $B_{qf}^{(Z)}(\alpha_i)$ are not indicated on the right sides of Eqs. (19) and (20). T_Z is the effective temperature of the DNS with the charge number Z of its light fragment:

$$T_Z(\ell, \alpha_i) = \sqrt{\frac{E_Z^*(\ell, \alpha_i)}{a}}, \tag{21}$$

where $a = A_{\rm CN}/12$ MeV^{-1}. The excitation energy $E_Z^*(\ell, \alpha_i)$ of the DNS with the charge Z and mass A numbers of the light fragment is determined by the difference between collision energy $E_{\rm c.m.}$ and peculiarities of the driving potential U_{dr} calculated for the given value of ℓ:

$$E_Z^*(\ell, \alpha_i) = E_{\rm c.m.} - V_{\rm min}(Z, A, R_m, \alpha_i) - \Delta Q_{gg}(Z, A), \tag{22}$$

where

$$\Delta Q_{gg}(Z, A) = B_P(Z_P, A_P) + B_T(Z_T, A_T) - (B_1(Z, A) + B_2(Z_c, A_c)) \tag{23}$$

is a change of the binding energy of the DNS fragments during its evolution from the initial value ($Z = Z_P$ and $A = A_P$) to the final configuration with the charge and mass numbers Z and A, respectively.

The fusion cross section is calculated by Eq. (2) and its some part corresponding to the range $\ell > \ell_B$ contributes to the fast fission cross section

$$\sigma_{\rm ffis}(E_{\rm c.m.}) = \sum_{\ell=\ell_B}^{\ell_d} \sigma_{\rm fus}(E_{\rm c.m.}, \ell), \tag{24}$$

where ℓ_d is the maximum value of the angular momentum leading to capture (DNS formation) at a given collision energy; ℓ_B is a value of ℓ at which the fission barrier of the compound nucleus disappears [25]. The fast fission is the fission of the rotating mononucleus into two fragments due to disappearance of its fission barrier B_f which depends on the angular momentum L and excitation energy $E_{\rm CN}^*$ [23]. The fast fission process does not allow the heated and rotating mononucleus to turn into a compound nucleus.

The results of averaging over all orientation angles α_T of the axis of axial symmetry of the target nucleus ^{232}Th in the interval $0^\circ \leqslant \alpha_T \leqslant 90^\circ$,

$$\sigma_{\rm fus}(E_{\rm c.m.}, \ell) = \int_0^{\pi/2} \sigma_{\rm cap}(E_{\rm c.m.}, \ell, \alpha_T) P_{CN}(E_{\rm c.m.}, \ell, \alpha_T) \times \sin\alpha_T d\alpha_T, \tag{25}$$

are used in calculations of the partial cross sections of the evaporation residue formation. Surface vibrations relative to the cores in the ground spherical state are taken into account if one of colliding nucleus (^{48}Ca) has spherical shape in its ground state. The procedure of the averaging over vibration states of the spherical shape has considered in [26].

The capture cross section is averaged over all orientation angles α_T in a similar way:

$$\sigma_{\rm cap}(E_{\rm c.m.}, \ell) = \int_0^{\pi/2} \sigma_{\rm cap}(E_{\rm c.m.}, \ell, \alpha_T) \sin\alpha_T d\alpha_T. \tag{26}$$

The partial cross section of complete fusion in the collision with the orientation angles α_i $(i = 1, 2)$ is calculated taking into account the hindrance to complete fusion caused by quasifission:

$$\sigma_{\rm fus}(E_{\rm c.m.}, \ell, \{\alpha_i\}) = \sigma_{\rm cap}(E_{\rm c.m.}, \ell, \{\alpha_i\}) \times P_{CN}(E_{\rm c.m.}, \ell, \{\alpha_i\}). \tag{27}$$

The theoretical values of the fusion probability to compare with the experimental data are found as a ratio of the total fusion and capture cross sections

$$P_{\rm CN}(E_{\rm c.m.}) = \frac{\sigma_{\rm fus}(E_{\rm c.m.})}{\sigma_{\rm cap}(E_{\rm c.m.})}, \tag{28}$$

where the total cross sections σ_i $(i =$ fus, cap) are calculated by summing the contributions of the partial waves leading to capture: $\ell = 0$—ℓ_d. The results of the calculation $P_{\rm CN}$ are presented in Fig. 5. Its maximum values are in the range $E_{\rm c.m} = 192$–205 MeV which is significantly higher than the Coulomb barrier $V_B = 184$ MeV which is shown in Fig. 2. This result is calculated for collisions with the orientation

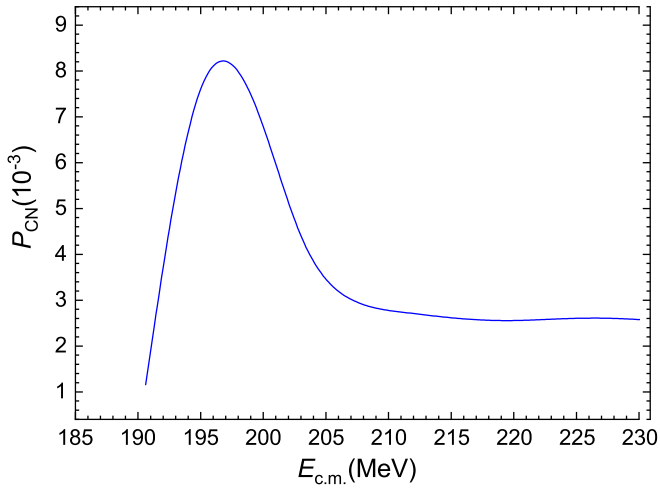

FIG. 5. Dependence of the probability of complete fusion (P_{CN}) on the collision energy in center of mass system for the reaction $^{48}Ca + ^{232}Th$.

angle $\alpha_T = 30^\circ$. The value of V_B is 198 MeV for the collisions with the orientation angle $\alpha_T = 90^\circ$. The difference between V_B calculated for small values of α_T and $E_{c.m.} = 197$ MeV corresponding to the maximum value of P_{CN} is an indication to the presence of the intrinsic barrier B^*_{fus}. The DNS should overcome this barrier during its evolution to be transformed into a compound nucleus. This means that B^*_{fus} causes hindrance to complete fusion and it increases events of the quasifission as the breakup of the DNS into two fragments due to small values of the quasifission barrier presented in Fig. 6.

The quasifission cross sections are calculated from the capture cross section by the expression

$$\sigma_{qf}(E_{c.m.}) = \sum_{\ell=0}^{\ell_d} \sigma_{cap}(E_{c.m.}, \ell)(1 - P_{CN}(E_{c.m.}, \ell)). \quad (29)$$

The results of calculated cross sections of the complete fusion by Eq. (2), quasifission by Eq. (29), and fast fission by Eq. (24)

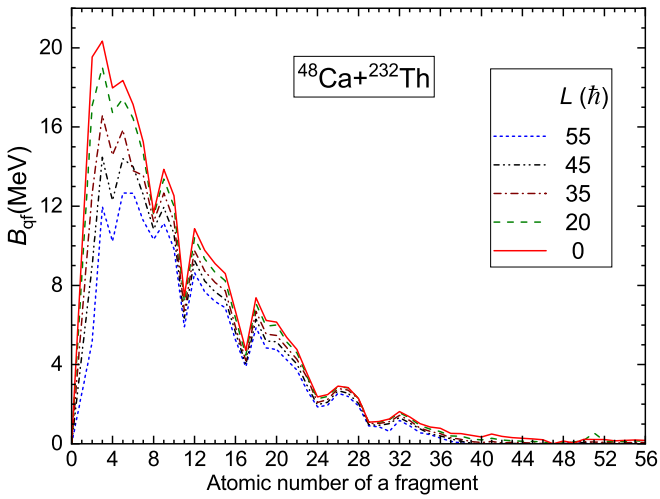

FIG. 6. Dependence of the DNS quasifission barrier B_{qf} on the charge of the light fragment in the reaction $^{48}Ca + ^{232}Th$.

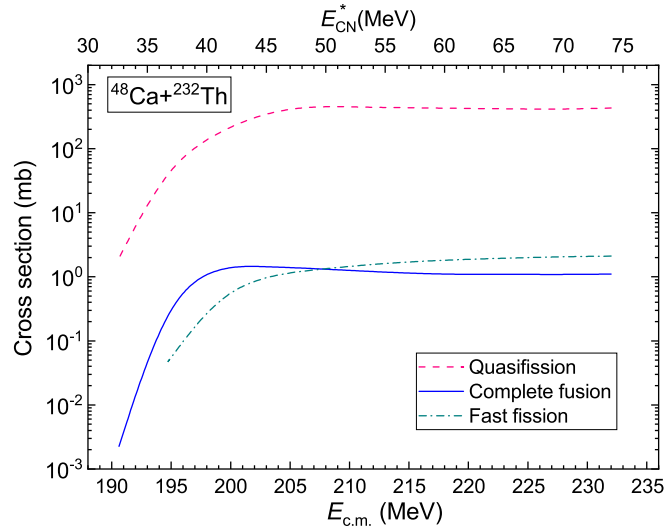

FIG. 7. Cross sections of the quasifission (dashed curve), complete fusion (solid curve), and fast fission (dot-dashed curve) calculated in this work for the reaction $^{48}Ca + ^{232}Th$.

for the reaction $^{48}Ca + ^{232}Th$ are presented in Fig. 7. As it is seen from this figure, the quasifission cross section is the dominant process and the capture cross section is determined by the quasifission cross section. The fusion cross section increases from small values up to large values in the optimal range is $E_{lab} = 230$–260 MeV. Then fast fission becomes dominant due to the fact that the inequality $\ell_f < \ell$ begins to hold. The fission barrier of the heated and rotating heavy nucleus decreases by increasing its orbital angular momentum. At a certain value of the orbital angular momentum, the fission barrier completely disappears, the mononucleus loses stability and disintegrates into two fragments [25]. The fission barrier of heavy elements ($Z > 106$) exists only due to the quantum shell effects of the nuclear structure. This kind of barrier decreases by the increase of the CN excitation energy [27,28]. The difference between fast fission and quasifission is a mononucleus undergoing rapid fission in a system that has survived against quasifission. According to the results obtained by the DNS model, the quasifission can occur for all values of its angular momentum $L_{DNS} = \ell_{DNS} \times h$. This is one of the main differences between fast fission and quasifission [17].

V. EVAPORATION RESIDUE CROSS SECTION

The partial cross sections of the CN formation $\sigma_{fus}(E_{c.m.}, \ell)$ determined by Eq. (25) are used in calculation of the partial cross sections of the evaporation residue formation. The excitation energy of the CN is determined by

$$E^*_{CN}(E_{c.m}, \ell) = E_{c.m} + Q_{gg} - V_{CN}(\ell), \quad (30)$$

where $Q_{gg} = B_1 + B_2 - B_{CN}$ is the energy balance of the reaction; B_1, B_2, and B_{CN} are the binding energies of the interacting nuclei and CN, which are taken from the table in Refs. [21,22]; $V_{CN}(\ell)$ is the CN rotational energy. The cross section of the evaporation residue formed after emission of x

neutrons is calculated as a sum of its partial cross sections:

$$\sigma_{ER}^{x}(E_x^*) = \sum_{0}^{\ell_d} \sigma_{ER}^{x}(E_x^*, \ell), \tag{31}$$

where $E_x^* = E_{\rm CN}^*(E_{\rm c.m}, \ell) - x\epsilon$; ϵ is the emission energy of a particle. For the given value of excitation energy and angular momentum, the partial cross section of ER formation obtained after the emission of neutrons was estimated by the formula [17,29]

$$\sigma_{ER}^{x}(E_x^*, \ell) = \sigma_{ER}^{x-1}(E_{x-1}^*, \ell) W_{\rm sur}^{x}(E_{x-1}^*, \ell). \tag{32}$$

When $x = 1$, in the right side of Eq. (32) we have $\sigma_{ER}^{0}(E_0^*, \ell)$ which corresponds to the fusion cross section $\sigma_{\rm fus}(E_{CN}^*, \ell)$ before neutron emission and $W_{\rm sur}(E_{\rm CN}^*, \ell)$ denotes the survival probability of the compound nucleus against fission during the de-excitation cascade. The survival probability $W_{\rm sur}^{x}(E_{x-1}^*, \ell)$ is calculated by the statistical model implanted in KEWPIE2 [30]. In the present work, the neutron emission width was calculated by the Weisskopf-Ewing model [31] and the fission-decay width is estimated within the standard Bohr-Wheeler transition-state model [32] (more details in Ref. [23]):

$$\Gamma_n = \frac{(2S_n + 1)\mu_n}{\pi^2\hbar^2} \int_0^{E_{CN}^* - B_n} \frac{\sigma_{\rm inv}^{n}(\epsilon_n)\rho_B(E_B^*)\epsilon_n d\epsilon_n}{\rho_{CN}(E_{CN}^*)}, \tag{33}$$

$$\Gamma_f^{BW} = \frac{1}{2\pi\,\rho_{CN}^{gs}(E_{CN}^*, J_{CN})} \int_0^{E_{CN}^* - B_f} \rho_C^{sd}(E_{sd}^*, J_{CN}) \times T_{\rm fiss}(\epsilon_f) d\epsilon_f. \tag{34}$$

In the calculation of the fission-decay width, the Hill-Wheeler transmission coefficient [33] was used as the penetration factor $T_{\rm fiss}(\epsilon_f)$, moreover, the effect of viscosity on the fission is processed as a Kramer correction factor [34], and the difference in the number of stationary collective states in the ground state and at the saddle point as a Strutinsky factor [35] were taken into account. Finally, the new combined fission-decay width expression was used as

$$\Gamma_f = K \cdot S \cdot \Gamma_f^{BW}, \tag{35}$$

where in the Kramer factor $K = \sqrt{1 + (\frac{\beta}{2\omega_{sd}})^2} - \frac{\beta}{2\omega_{sd}}$, β is reduced friction parameter and its value set to $5.0\,{\rm zs}^{-1}$; in the Strutinsky factor $S = \frac{\hbar\omega_{gs}}{T_{gs}}$, $\hbar\omega_{gs} = 1$ MeV, and T_{gs} is nuclear temperature within the Fermi-gas model.

The dependence of the fission barrier B_f on the excitation energy $E_{\rm CN}^*$ is taken into account at calculations of the survival probability $W_{\rm sur}$:

$$B_f = B_{\rm LSD} - f\delta W, \tag{36}$$

where $B_{\rm LSD}$ and δW are the empirical fission-barrier which is calculated by the Lublin-Strasbourg drop model [36] and the effective shell-correction energy, respectively. The ground-state shell correction energies and the parametrizations for the empirical fission-barrier $B_{\rm LSD}$ use the mass table of Möller *et al.* [22]. The dependence of the fission barrier on the excitation energy $E_{\rm CN}^*$ and angular momentum ℓ of the CN can be taken into account as in Ref. [12], where the correction factor was written as $f = h(T) \cdot q(\ell)$,

$$h(T) = \{1 + \exp[(T - T_0)/d]\}^{-1}, \tag{37}$$

and

$$q(\ell) = \{1 + \exp[(\ell - \ell_{1/2})/\Delta\ell]\}^{-1}. \tag{38}$$

In Eq. (37) $T = \sqrt{E_{CN}^*/a}$ is nuclear temperature, $d = 0.3$ MeV is the rate of washing out the shell corrections with the temperature, $T_0 = 1.16$ MeV is the value at which the damping factor $h(T)$ is reduced by 1/2; in Eq. (38), $\Delta\ell = 3\hbar$ is the rate of washing out the shell corrections with the angular momentum, $\ell_{1/2} = 20\hbar$ is the value at which the damping factor $q(\ell)$ is reduced by 1/2.

The level-density parameter has been taken from the work Nerlo-Pomorska *et al.* [37] and it can be expressed in the following form:

$$a = 0.092A + 0.036A^{2/3}\mathfrak{B}_s + 0.275A^{1/3}\mathfrak{B}_k - 0.00146\frac{Z^2}{A^{1/3}}\mathfrak{B}_c, \tag{39}$$

where $\mathfrak{B}_s$ is the surface term, $\mathfrak{B}_k$ is the curvature term, and $\mathfrak{B}_c$ is the Coulomb term for a deformed nucleus [38].

The shell-correction effects decrease as the excitation energy rises. To incorporate this damping effect, Ignatyuk's prescription [39] was used in the calculation, which considers the level density parameter to be dependent on the excitation energy. In the ground state, one has the following explicit expression:

$$a_{gs}(E_x^*) = a\left[1 + (1 - e^{-E_x^*/E_d})\frac{\Delta E_{sh}}{E_x^*}\right], \tag{40}$$

where the default value of the shell-damping energy E_d has been fixed at 19.0 MeV. All models and parameters, which are used in the calculation of survival probability, are based on of our previous calculations of the decay for the different reactions [23,26,40].

VI. DESCRIPTION OF THE EXPERIMENTAL RESULTS OF SYNTHESIS OF DS IN HOT FUSION REACTION

The evaporation residue cross sections of the 3*n*, 4*n*, and 5*n* de-excitation channels have been calculated by Eq. (1). The survival probability $W_{\rm sur}$ of the heated and rotating CN is calculated by the statistical model implanted in KEWPIE2 [30], which is dedicated to the study of the evaporation residues at the synthesis of SHE. A maximum of the evaporation residue cross section was observed for the 4*n* channel at $E_{\rm lab} = 237.5$ MeV which corresponds to $E_{\rm CN}^* = 40$ MeV of the CN excitation energy. Comparison of the theoretical results of this work with the measured data in Ref. [14] shows a good description of the experimental data (see Fig. 8). It is interesting to establish reasons causing such a strong difference (20 times) between the measured cross sections of the isotopes of Ds in the cold fusion ^{64}Ni + ^{208}Pb and hot fusion ^{48}Ca + ^{232}Th reactions. Table I presents comparison of the measured ER cross sections $\sigma_{\rm ER}$, excitation energy

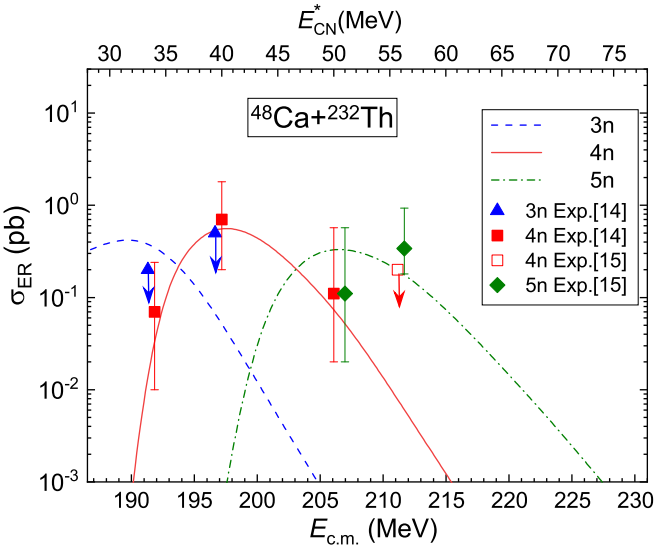

FIG. 8. Comparison of the ER cross sections of the de-excitation $3n$ (dashed curve), $4n$ (solid curve), and $5n$ (dot-dashed curve) channels calculated in this work with the experimental data of the $3n$ (triangles) and $4n$ (solid squares) channels obtained in Ref. [14] and of the $4n$ (open square) and $5n$ (diamonds) obtained in Ref. [15] of the de-excitation of the heated and rotating CN formed in the ^{48}Ca + ^{232}Th reaction. The symbols with arrows show the upper cross-section limits.

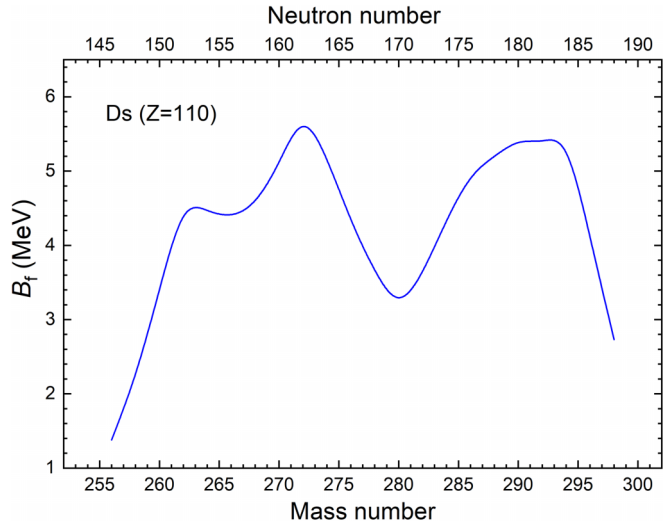

FIG. 9. Fission barrier B_f for darmstadtium ($Z = 110$) obtained from [41] as a function of the mass and neutron numbers.

E^*_{CN} corresponding to the measured data, and fission barrier B_f of the CN calculated in Refs. [41,42], as well as fusion probability P_{CN} for the cold fusion ^{64}Ni + ^{208}Pb (from [11]) and hot fusion ^{48}Ca + ^{232}Th (this work) reactions.

The main strong effect causing the large difference in the measured ER cross sections for the above mentioned reactions is a difference in the fission barrier providing the stability against fission. The fission barrier of the Ds isotopes is very sensitive to the neutron number due to the shell effects of its proton and neutron subsystems. Figure 9 shows the dependence of the fission barrier B_f on the mass and neutron numbers for the Ds isotopes. The isotopes ^{272}Ds and ^{280}Ds are formed as a CN in the ^{64}Ni + ^{208}Pb and ^{48}Ca + ^{232}Th reactions, respectively. The neutron number of ^{272}Ds is equal to magic number 162 for neutrons, consequently, the fission barrier has a maximum value. The small value of the excitation $E^*_{CN} = 12.7$ MeV is favorable for the survival probability W_{sur} and the ER cross section is large $\sigma_{ER} = 15$ pb in spite of the small fusion probability 10^{-5} [11].

TABLE I. The measured ER cross sections, excitation energy E^*_{CN} corresponding to the measured data, and fission barrier B_f of the CN calculated in Ref. [41], as well as fusion probability P_{CN} for the cold fusion ^{64}Ni + ^{208}Pb (from [11]) and hot fusion ^{48}Ca + ^{232}Th (this work) reactions.

Reaction	σ_{ER} (pb)	E^*_{CN} (MeV)	B_f MeV	P_{CN}
^{64}Ni + ^{208}Pb	15^{+9}_{-6}	12.7	5.62	10^{-5}
^{48}Ca + ^{232}Th	$0.7^{+1.1}_{-0.5}$	40.37	3.29	8.3×10^{-3}

The neutron number ($N = 170$) of ^{280}Ds is between two magic numbers 162 and 184 for the neutron subsystem. Therefore, the fission barrier has a minimum value (see Fig. 9). As a result the survival probability W_{sur} is very small for the excitation energies $E^*_{CN} = 40.37$ MeV.

The decrease of the neutron numbers due to evaporation neutrons from ^{280}Ds in competition with the fission process leads to an increase of the fission barrier. Therefore, a formation of the isotope ^{276}Ds formed in the $4n$ de-excitation channel has relatively large cross section in comparison with the $2n$ and $3n$ channels. The measured ER cross section of the $5n$ channel is lower than the $4n$ channel since the fission barrier decreases with an increase of the excitation energy E^*_{CN}.

VII. CONCLUSIONS

The ER cross section of at the synthesis of ^{276}Ds by the $3n$, $4n$, and $5n$ de-excitation channels in the ^{48}Ca + ^{232}Th reactions has been calculated and the results of this work is compared with the recent experimental from Refs. [14,15] obtained in the SHE factory at JINR (Dubna, Russia). The maximal value 0.7 pb of the ER cross section was observed for the $4n$ channel. In spite of the large probability of the CN formation in this reaction, the ER cross section is much smaller (20 times) than the experimental data obtained in the cold fusion reactions ^{64}Ni + ^{208}Pb for the $1n$ channel by Hofmann *et al.* [43]. This fact is explained by the dependence of the fission barrier B_f on the mass number A for the given element Ds ($Z = 110$). The isotopes ^{272}Ds and ^{280}Ds are formed as a CN in the ^{64}Ni + ^{208}Pb and ^{48}Ca + ^{232}Th reactions, respectively. The neutron number of ^{272}Ds is equal to magic number 162 for neutrons, consequently, the fission barrier has a maximum value. The small value of the excitation $E^*_{CN} = 12.7$ MeV is favorable for the survival probability W_{sur} and the ER cross section is large $\sigma_{ER} = 15$ pb in spite of the small fusion probability 10^{-5} [11]. The neutron number ($N = 170$) of ^{280}Ds is between two magic numbers 162 and

184 for the neutron subsystem. The decrease of the fission barrier B_f at large excitation energies causes a smallness of the ER cross section of xn channels with $x > 4$ in hot fusion reactions.

[1] S. Hofmann and G. Münzenberg, Rev. Mod. Phys. **72**, 733 (2000).
[2] P. Armbruster, Annu. Rev. Nucl. Part. Sci. **50**, 411 (2000).
[3] K. Morita, K. Morimoto, D. Kaji, T. Akiyama, S.-i. Goto, H. Haba, E. Ideguchi, R. Kanungo, K. Katori, H. Koura, H. Kudo, T. Ohnishi, A. Ozawa, T. Suda, K. Sueki, H. Xu, T. Yamaguchi, A. Yoneda, A. Yoshida, and Y. Zhao, J. Phys. Soc. Jpn. **73**, 2593 (2004).
[4] Y. Oganessian, J. Phys. G: Nucl. Part. Phys. **34**, R165 (2007).
[5] N. V. Antonenko, E. A. Cherepanov, A. K. Nasirov, V. P. Permjakov, and V. V. Volkov, Phys. Rev. C **51**, 2635 (1995).
[6] G. G. Adamian, N. V. Antonenko, and W. Scheid, Nucl. Phys. A **678**, 24 (2000).
[7] V. Zagrebaev and W. Greiner, Phys. Rev. C **78**, 034610 (2008).
[8] N. Wang, E.-G. Zhao, W. Scheid, and S.-G. Zhou, Phys. Rev. C **85**, 041601(R) (2012).
[9] J. Hong, G. G. Adamian, and N. V. Antonenko, Phys. Lett. B **764**, 42 (2017).
[10] Y. T. Oganessian, V. K. Utyonkov, S. N. Dmitriev, Y. V. Lobanov, M. G. Itkis, A. N. Polyakov, Y. S. Tsyganov, A. N. Mezentsev, A. V. Yeremin, A. A. Voinov, E. A. Sokol, G. G. Gulbekian, S. L. Bogomolov, S. Iliev, V. G. Subbotin, A. M. Sukhov, G. V. Buklanov, S. V. Shishkin, V. I. Chepygin, G. K. Vostokin, N. V. Aksenov, M. Hussonnois, K. Subotic, V. I. Zagrebaev, K. J. Moody, J. B. Patin, J. F. Wild, M. A. Stoyer, N. J. Stoyer, D. A. Shaughnessy, J. M. Kenneally, P. A. Wilk, R. W. Lougheed, H. W. Gäggeler, D. Schumann, H. Bruchertseifer, and R. Eichler, Phys. Rev. C **72**, 034611 (2005).
[11] G. Giardina, S. Hofmann, A. I. Muminov, and A. K. Nasirov, Eur. Phys. J. A **8**, 205 (2000).
[12] G. Giardina, G. Mandaglio, A. K. Nasirov, A. Anastasi, F. Curciarello, and G. Fazio, Nucl. Phys. A **970**, 169 (2018).
[13] W. Loveland, Eur. Phys. J. A **51**, 120 (2015).
[14] Y. T. Oganessian, V. K. Utyonkov, M. V. Shumeiko, F. S. Abdullin, S. N. Dmitriev, D. Ibadullayev, M. G. Itkis, N. D. Kovrizhnykh, D. A. Kuznetsov, O. V. Petrushkin, A. V. Podshibiakin, A. N. Polyakov, A. G. Popeko, I. S. Rogov, R. N. Sagaidak, L. Schlattauer, V. D. Shubin, D. I. Solovyev, Y. S. Tsyganov, A. A. Voinov, V. G. Subbotin, N. S. Bublikova, M. G. Voronyuk, A. V. Sabelnikov, A. Y. Bodrov, Z. G. Gan, Z. Y. Zhang, M. H. Huang, and H. B. Yang, Phys. Rev. C **108**, 024611 (2023).
[15] Y. T. Oganessian, V. K. Utyonkov, M. V. Shumeiko, F. S. Abdullin, G. G. Adamian, S. N. Dmitriev, D. Ibadullayev, M. G. Itkis, N. D. Kovrizhnykh, D. A. Kuznetsov, O. V. Petrushkin, A. V. Podshibiakin, A. N. Polyakov, A. G. Popeko, I. S. Rogov, R. N. Sagaidak, L. Schlattauer, V. D. Shubin, D. I. Solovyev, Y. S. Tsyganov, A. A. Voinov, V. G. Subbotin, N. S. Bublikova, M. G. Voronyuk, A. V. Sabelnikov, A. Y. Bodrov, N. V. Aksenov, A. V. Khalkin, Z. G. Gan, Z. Y. Zhang, M. H. Huang, and H. B. Yang, Phys. Rev. C **109**, 054307 (2024).
[16] S. Hofmann, Rep. Prog. Phys. **61**, 639 (1998).
[17] A. Nasirov, A. Fukushima, Y. Toyoshima, Y. Aritomo, A. Muminov, S. Kalandarov, and R. Utamuratov, Nucl. Phys. A **759**, 342 (2005).
[18] G. G. Adamian, R. V. Jolos, A. K. Nasirov, and A. I. Muminov, Phys. Rev. C **56**, 373 (1997).
[19] A. B. Migdal, *Theory of the finite fermi systems and properties of atomic nuclei* (Nauka, Moscow, 1983) .
[20] E. C. Kemble, Phys. Rev. **48**, 549 (1935).
[21] G. Audi, A. H. Wapstra, and C. Thibault, Nucl. Phys. A **729**, 337 (2003).
[22] P. Moller, J. Nix, W. Myers, and W. Swiatecki, At. Data Nucl. Data Tables **59**, 185 (1995).
[23] B. M. Kayumov, O. K. Ganiev, A. K. Nasirov, and G. A. Yuldasheva, Phys. Rev. C **105**, 014618 (2022).
[24] A. K. Nasirov, B. M. Kayumov, G. Mandaglio, G. Giardina, K. Kim, and Y. Kim, Eur. Phys. J. A **55**, 29 (2019).
[25] A. J. Sierk, Phys. Rev. C **33**, 2039 (1986).
[26] A. Nasirov and B. Kayumov, Phys. Rev. C **109**, 024613 (2024).
[27] K. Kim, Y. Kim, A. K. Nasirov, G. Mandaglio, and G. Giardina, Phys. Rev. C **91**, 064608 (2015).
[28] G. Mandaglio, A. K. Nasirov, A. Anastasi, F. Curciarello, G. Fazio, and G. Giardina, Nucl. Phys. A **979**, 204 (2018).
[29] G. Mandaglio, G. Giardina, A. K. Nasirov, and A. Sobiczewski, Phys. Rev. C **86**, 064607 (2012).
[30] H. Lü, A. Marchix, Y. Abe, and D. Boilley, Comput. Phys. Commun. **200**, 381 (2016).
[31] V. Weisskopf, Phys. Rev. **52**, 295 (1937).
[32] N. Bohr and J. A. Wheeler, Phys. Rev. **56**, 426 (1939).
[33] D. L. Hill and J. A. Wheeler, Phys. Rev. **89**, 1102 (1953).
[34] H. Kramers, Physica **7**, 284 (1940).
[35] V. Strutinsky, Phys. Lett. B **47**, 121 (1973).
[36] F. A. Ivanyuk and K. Pomorski, Phys. Rev. C **79**, 054327 (2009).
[37] B. z. Nerlo-Pomorska, K. Pomorski, and J. Bartel, Phys. Rev. C **74**, 034327 (2006).
[38] R. W. Hasse and W. D. Myers, *Geometrical Relationships of Macroscopic Nuclear Physics* (Springer, Berlin/Heidelberg, 1988).
[39] A. V. Ignatyuk, G. N. Smirenkin, and A. S. Tishin, Sov. J. Nucl. Phys. **21**, 485 (1975).
[40] A. Nasirov, B. Kayumov, O. Ganiev, and G. Yuldasheva, Phys. Lett. B **842**, 137976 (2023).
[41] M. Kowal, P. Jachimowicz, and A. Sobiczewski, Phys. Rev. C **82**, 014303 (2010).
[42] P. Jachimowicz, M. Kowal, and J. Skalski, At. Data Nucl. Data Tables **138**, 101393 (2021).
[43] S. Hofmann, V. Ninov, F. P. Heßberger, P. Armbruster, H. Folger, G. Münzenberg, H. J. Schött, A. G. Popeko, A. V. Yeremin, A. N. Andreyev, S. Saro, R. Janik, and M. Leino, Z. Phys. A Hadrons and Nuclei **350**, 277 (1995).